Characteristics and durability of alkali activated Egyptian blast-furnace slag-silica fume pastes

Article · January 2014

CITATIONS
0

READS
130

4 authors:

Mohamed Heikal
Benha University
141 PUBLICATIONS **1,442** CITATIONS
SEE PROFILE

Mostafa Y Nassar
Benha University
50 PUBLICATIONS **698** CITATIONS
SEE PROFILE

Gamal El-Sayed
Benha University
57 PUBLICATIONS **628** CITATIONS
SEE PROFILE

S.M. Ibrahim
Benha University
5 PUBLICATIONS **30** CITATIONS
SEE PROFILE

Journal of Basic and Environmental Sciences 1 (2014) 119 - 135 ISSN 2356-6388

Characteristics and durability of alkali activated Egyptian blast-furnace slag-silica fume pastes

Mohamed Heikal,[a,b,*] M.Y. Nassar [a], G. El-Sayed [a], and S.M. Ibrahim[a]

[a] Chemistry Department, Faculty of Science, Benha University, Benha, Egypt,
[b] Chemistry Department, College of Science, Al Imam Mohammad Ibn Saud Islamic University (IMSIU), P.O Box 90950 Riyadh 11623, KSA, Fax: 009662591678.

Article Information

Received; 20 March. 2014
In Revised form; 12 April. 2014
Accepted; 12 April. 2014

Keywords:
Alkaline activation,
Electrical conductivity,
Thermal analysis,
Phase composition,
Microstructure

Abstract

Blast-furnace slag (GBFS) and silica fume (SF) are produced as by-product from chemical industries with limited recycling facility. This paper represents an experimental study aimed to produce cementless binding material using both of sodium hydroxide (SH) and waterglass liquid (SSL) as alkaline activator. The alkaline activation of GBFS-SF has been studied by using electrical conductivity, FT-IR, DTA/TGA, XRD and SEM techniques. As the hydration time increases the amount of hydration products increase. The chemically combined water and combined slag contents increase with curing ages. SEM images showed the presence of C-S-H and (N,C)-A-S-H gel with low porosity. The alkali activated GBFS-SF pastes are more durable in 5% $MgSO_4$ or 5% $MgCl_2$ solution than ordinary Portland cement (OPC) up to 180 days. The total chloride and total sulphate contents decrease with alkali activated GBFS-SF due to the formation of hydrated products, which fill the available open pores, thereby inhibit Cl^- or SO_4^{2-} ions penetration; this effect leads to a decreased accessibility of Cl^- or SO_4^{2-} ions towards the more dense close structure with low capillary pore structure.

1. Introduction

The last few years have shown extensive construction of cement factories in Egypt. The cement industry is considered as non-friendly environmental industry due to the continuous emission of CO_2 and quarrying of raw materials (limestone and clay) accompanying the fabrication process. Many researchers are working on this serious issue created by cement and one of the solutions is the introduction of polymeric inorganic cements by the development of inorganic aluminasilicate binders. A binder can be obtained by the reaction of industrial by-products such as fly ash (FA), silica fume (SF), and GBFS with the alkali activated solution. Depending on the nature of the raw materials to be activated, different reaction products are developed which have different microstructures. In the alkali activation of GBFS, the main reaction product is a hydrated calcium silicate hydrates (C-S-H gel), while in the activation of FA, the reaction product obtained is an inorganic polymer of amorphous nature formed by hydrated aluminosilicate chains 'geapolymer' [1].

GBFS is a by-product of the manufacturing of iron in a blast-furnace where iron ore, limestone and coke are heated up to 1500 ^oC. When these materials melt in the blast-furnace, two products are produced–molten iron, and molten slag. The molten slag is lighter and floats on the top of the molten iron. The molten slag comprises mostly silicates and alumina from the original iron ore, combined with some oxides from the limestone. The process of granulating the slag involves cooling

mode of the molten slag through high-pressure water jets. This rapidly quenches the slag forms granular particles. The rapid cooling prevents the formation crystal lattices, and the resulting granular material comprises non-crystalline calcium-aluminosilicates [2]. The granulated slag is further processed by drying and then ground to a very fine powder (GBFS).

Microsilica or simply silica fume is a by-product of the manufacture of silicon or of various silicon alloys by reducing quartz to silicon in an induction arc furnace at temperatures up to 2000^{o}C. Gasified SiO_2 at high temperatures condenses in the low-temperature zone to tiny spherical particles consisting of non-crystalline silica. Chemical composition of SF depends not only upon the raw materials used, but also upon the quality of electrodes and the purity of silicon product. The impurities in SF decrease as the amount of silicon increases in the final products. SF contain 85-95% non-crystalline silica. Minor components in SF are 0.1–0.5% Al_2O_3, 0.1–5% Fe_2O_3, 2–5% carbon, 0.1–0.2% S, less than 0.12% CaO, less than 0.1% TiO_2, less than 0.07% P_2O_5 and less than 1% alkalis [3]. Its particle has an average diameter in the order of 0.1μm, and surface areas in the range 20-25m^2/g. SF dissolves rapidly in $Ca(OH)_2$(CH) saturated solution and is highly pozzolanic. Because of its small particles and highly reactivity, SF is often used as a component of densely packed cementing materials, including alkali-activated cements, with high strength and low permeability [4].

The reaction mechanism of aluminosilicates containing a calcium bearing compound differs from the geopolymeric reaction as explained. It has also been reported that the type of calcium bearing compound in the starting material plays an important role in the alkali activation aluminosilicate materials. Alkalis first attack aluminosilicate particles breaking the outer layer, and then a polycondensation of reaction products takes place. Wang et.al. [5] Suggested that though the initial reaction products form due to dissolution and precipitation. At later ages, a solid state mechanism is followed where the reaction takes place on the surface of the formed particles, dominated by slow diffusion of the ionic species into the unreacted core. Alkali cation (M^+) acts as a catalyst for the reaction in the initial stages of hydration, via cation exchange with the Ca^{2+} ions [6,7]. The alkaline cations act as structure creators. The nature of the anion in the solution also plays a determining role inactivation, particularly in early ages and especially with regard to paste setting [8,9]. The final products of the slag reaction are similar to the products of cement hydration(C-S-H); the major difference being the rate and intensity of the reaction. It has also been observed that the alkalis are bound to the reaction products and are not freely a available in the pore solution (this depends on the alkali concentration used, though), thereby negating the potential for alkali-silica reactivity. This paper represents experimental trials of alkali activated blast-furnace slag-silica fume to produce cementless binding material.

2. Experimental techniques:

2.1. Materials:

2.1.1. Egyptian blast-furnace slag:

Blast-furnace slag (GBFS) was provided from Iron and Steel Company, Helwan Governorate, Egypt. Its chemical oxide composition is given in Table 1.

Table 1: Chemical composition of starting materials, mass %.

Oxide composition (%)	GBFS	SF	SRC	SSL
SiO_2	37.81	99.93	21.40	30.7
Al_2O_3	13.14	0.48	3.67	--
Fe_2O_3	0.23	2.8	5.05	--
CaO	38.70	0.90	64.03	--
MgO	7.11	0.0	1.50	--
SO_3	1.19	0.0	2.05	--
Na_2O	1.03	0.0	0.30	10.3
K_2O	0.19	0.64	0.22	--
TiO_2	0.34			--
P_2O_5	0.16			--
L.O.I	0.00	0.50	1.60	59.0
Total	99.90	104.71	99.82	100.0

XRD patterns, FTIR spectra and SEM are shown in Figs 1-3. Blaine surface area of slag was ≈ 4500±50 cm^2/g. The diffraction patterns of GBFS were shown in Fig. 1. The XRD pattern indicates that GBFS is an amorphous material, which can be observed that there is a broad diffuse hump peak in the region of 20–38° 2θ suggesting that the GBFS consists of

glassy phases. Fig. 2 represent FTIR spectra of GBFS. It contains two main bands at 484.93 and 967cm^{-1} as well as two bands less intense at 697.79 and 1422 cm^{-1}. Bands at 967 and 484.93 cm^{-1} imply the presence of orthosilicate units $[Si_2O_7]^{6-}$ with partial substitution of Si^{4+} by Al^{3+} in tetrahedral positions. These units are built of two silicooxygen (or silico/and aluminooxygen) tetrahedra, connected with oxygen bridge. The two bands at 967 and 484.93 cm^{-1} represent the internal vibrations of $[SiO_4]^{4-}$ and $[AlO_4]^{5-}$ tetrahedral. The first comes from Si(Al)–O asymmetric stretching vibrations; the second should be assigned to O–Si–O bonds bending vibration. The appearance of the most intense band at relatively low wave numbers proves that, the silicate phases occurring in the GBFS containing orthosilicate units $[Si_2O_7]^6$. The existence of the weak band at 697.79 cm^{-1}, assigned to the symmetric stretching vibrations of the Si–O–Si(Al) bridges, further confirms the presence of these units. It is possible to suppose that, it is also connected with vibrations of Si–O–Al bridges, formed by linkage of $[SiO_4]^{4-}$ and $[AlO_4]^{5-}$ tetrahedral. The most intense band at 967 cm^{-1} proves the significant content of glassy phase in the structure of GBFS. GBFS particle morphologies obtained using SEM is shown in Fig. 3. GBFS is composed of angular particles of varying sizes. This material presents a mean particle size of about 12µm and irregular shape morphology with a dense-compact structure.

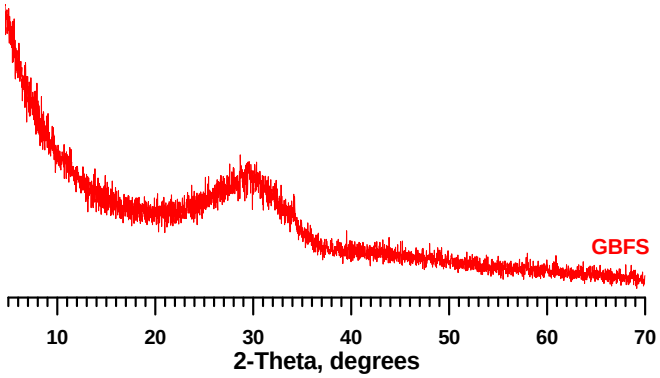

Fig1: XRD pattern of GBFS.

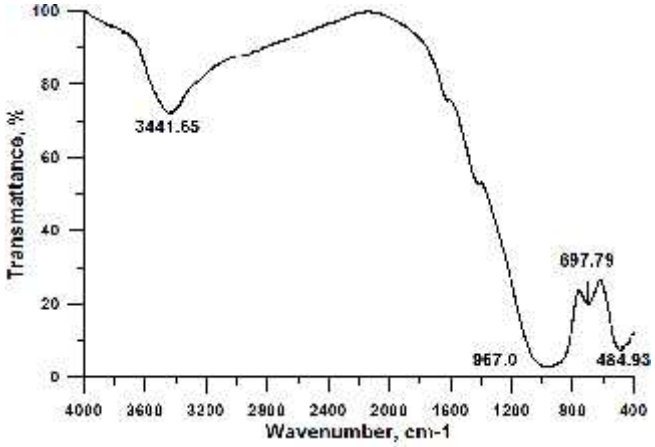

Fig 2: FTIR spectra of GBFS.

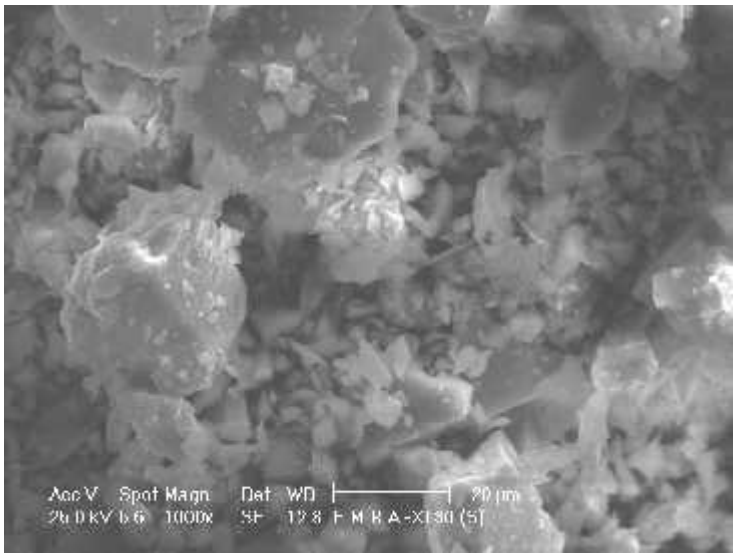

Fig 3: SEM of GBFS.

2.1.2. Condensed silica fume:

Condensed silica fume (SF) is a by-product of silicon or ferrosilicon alloys industries, Egypt. Its particles have an average diameter of ≅ 0.1μm. The chemical analysis is given in Table 2. XRD patterns, FT-IR spectra and SEM are shown in Figs 4-6. XRD pattern of SF is shown in Fig. 4. SF is completely amorphous; exhibiting only a very broad scattering peak. FT-IR

spectra of SF shows the stronger absorbance bands at 1119.71, 807.78 and 480.61cm^{-1}, characteristic of absorption bands of condensed silica (Fig. 5). The broad band centered at 1119.71 cm^{-1} is attributed to asymmetric stretching frequency of Si-O-Si, the band centered at 807.78 cm^{-1} is due to symmetric stretching of Si-O-Si, and the band at 480.61 cm^{-1} is due to the bending frequency of O-Si-O [10].SF particles are densely packed with sphere like particles, and individual particles (Fig. 6) [11]. The Blaine surface area of SF is 20.90 m^2/g.

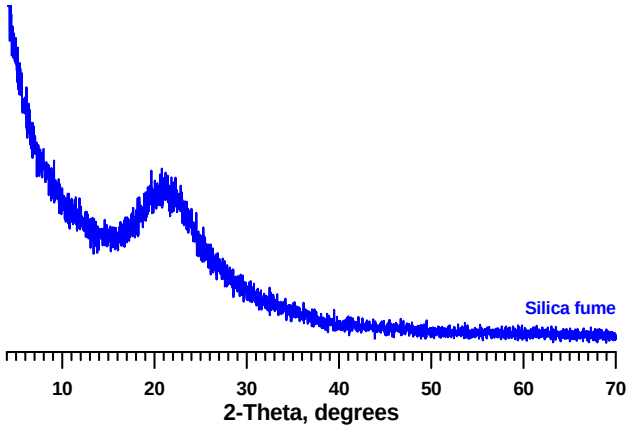

Fig 4**:** XRD pattern of Silica fume (SF).

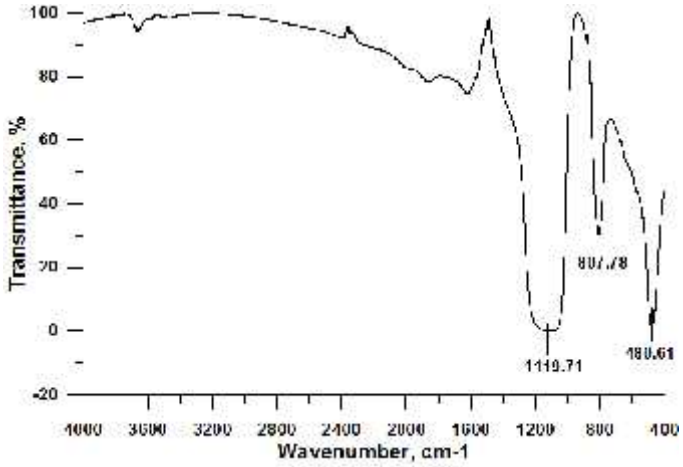

Fig 5: FT-IR spectra of Silica fume (SF).

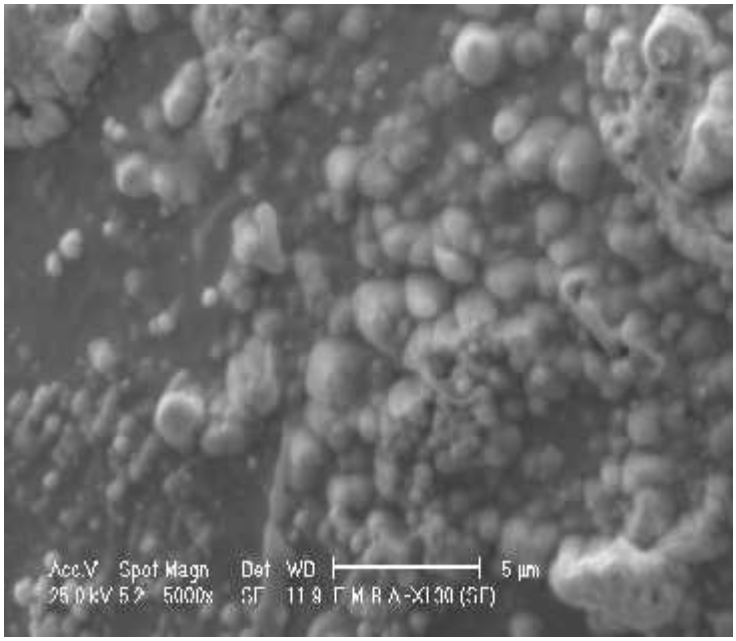

Fig 6: SEM of SF.

2.1.3. Sodium silicate liquid and sodium hydroxide:

NaOH was produced by SHIDO Company with purity 99%.Sodium silicate liquid (SSL) was provided from Islamic Silicate Industry, Badr City, Helwan. Sodium silicate liquid that consists of 30.7% SiO_2, 10.3% Na_2O and 59% H_2O with silica modulus SiO_2/Na_2O equal 2.98 and density 1.44 g/cm^3 is used. Sodium silicate solutions were used as activators and caustic soda content was increased by the addition of sodium hydroxide (NaOH) pellets.

The mix compositions were prepared as shown in Table 2. The ingredients of each mix were blended in a porcelain ball mill for one hour using a mechanical roller mill to ensure complete homogeneity. GBFS and SF were placed on smooth, non-absorbent surface, a crater was formed in the center and the mixing water with the activator was poured into the crater as shown in Table 2. The mixing process was performed according to ASTM specification [12]. The mixture was slightly

troweled to absorb the water for about 1 min, and then completed by vigorous mixing for 3 min. The pastes were moulded in one inch cubic moulds, then strong manually pressed into the moulds. The surface of the paste was then smoothed by thin edged trowel. Immediately after moulding, the specimens were cured in 100% RH at 35 ^{o}C for 24 h, then demoulded and cured in the humidifier up to 3 days, then cured under tap water after 3 days up to 90 days. For the specimens which were tested for the resistivity against 5% magnesium sulphate and 5% magnesium chloride as aggressive attack solution, the specimens were cured up to 7 days (zero time) in tap water then immersed in the aggressive solution 5% $MgSO_4$ or $MgCl_2$ up to 180 days. The aggressive solution was renewed monthly to maintain constant concentration.

Table 2: Composition of the investigated mixes containing alkaline activator (SiO_2 + Na_2O), mixing with 1kg of GBFS-SF.

Mix No.	GBFS	SF	SiO_2 mol/kg of GBFS	Na_2O (mol/kg of GBFS	H_2O (mL/kg of GBFS)
M0	100	0	0.50	0.75	300
M1	98	2	0.50	0.75	300
M2	96	4	0.50	0.75	300
M3	92	8	0.50	0.75	300

In electrical conductivity measurements, the co-axial cell type was used; it included concentric inner and outer electrodes mounted on an insulated base plate as shown in Fig. 7. The electrodes were polished before the experiment [13,14]. The mixing was done with the required amount of water that gives normal consistency in the presence of suitable amount of alkaline activator (SiO_2/Na_2O mol/kg). The measurements of the electrical conductivity were begun exactly three minutes after mixing with water (0 time). The pastes were placed in the space between the electrodes. The cell was kept in a cabinet chamber at 100% relative humidity during the test period from 3 minutes up to 28 days. The electrical conductivity was measured at 35^{o}C. The electrodes were connected with RLC meter, model SR-720. All data of the electrical conductivity were measured during the setting and hardening at relativity low AC frequency 1V and 1000Hz for resistance measurements.

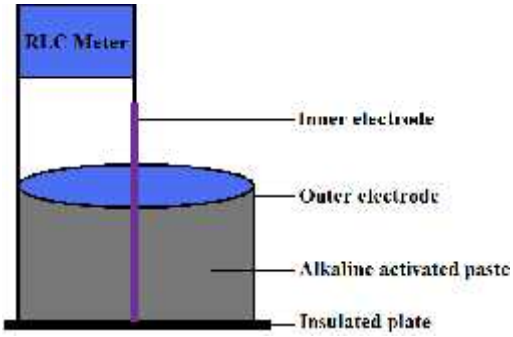

Fig 7: Electrical conductivity cell.

The compressive strength was done on a compression machine of SEIDNER, Riedinger, Germany, with maximum capacity of 600 KN force. The compressive strength was carried out on four samples as described by ASTM Specifications (ASTM Designation: C-150, 2007). The bulk density was carried out before the pastes subjected to compressive strength determination through weighing the hardened pastes (suspended in water) and in air (saturated surface dry). Each measurement was conducted on at least three similar cubes of the same age [15]. After, the determination of bulk density, four cubes of the same age were dried in a furnace at 105^{o}C for 24 hours then weighed after cooling in a desiccator. The total porosity of the cement pastes could be calculated [15].

The hydration of cement pastes were stopped by pulverizing 10g of representative sample in a beaker containing methanol–acetone mixture (1:1), then mechanically stirred for one hour. The mixture was filtered through a gooch crucible, G_4 and washed several times with the stopping solution then with ether. The solid was dried at 70 ^{o}C for one-hour complete evaporation of alcohol then collected in polyethylene bags; sealed and stored in desiccators for analysis [15]. The combined water content (W_n) considered as the percent of ignition loss of the dried samples (on the ignited weight basis). Approximately 2g of the predried sample were gradually ignited up to 800^{o}C for 1 hour soaking time. The results of combined water were corrected form the water of free lime present in each sample [15].

Free slag content determined according to the methods reported in earlier publication [16]. 1g sample is treated with 5g salicylic acid, 70 ml acetone and 30 ml methanol. After the mixture has been stirred (1 hour, magnetic stirrer), the resulting

solution is stored for 24 hours in an airtight container. The solution is then filtered on a G_4 glass filter and the filter residue is washed with 200ml methanol. The residue obtained is dried at 45 ^oC for 24 hours, and then heated at 800 ^oC for 20 minutes in an electrical furnace. These burning conditions are selected so that oxidation of slag constituents is largely avoided. The residue from the solution is weighed after the crucible has been cooled in desiccator. Corrections were made for neat slag and neat OPC and the loss of ignition of pozzolanic cement at 800 ^oC [17].

Thermal gravimetric analysis (TGA) was carried out using DTA-50 Thermal Analyzer (Schimadzu Co., Tokyo, Japan). A dried sample of about 50 mg (−53 μm) was used at heating rate 20 °C/min under nitrogen atmosphere. For IR spectroscopic investigation, the samples were prepared using alkali halide KBr pressed disk technique. The IR analysis was recorded from KBr disks using Gensis FT-IR spectrometer in the range 400–4000 cm^{-1} after 256 scans at 2 cm^{-1} resolution.

The scanning electron microscope (SEM) was taken with Inspect S (FEI Company, Holland) equipped with an energy dispersive X-ray analyzer (EDX). SEM was used to examine the microstructure of the fractured composites at the accelerating voltage of 200–30 kV and Power zoom magnification up to 300,000×. The samples are firstly dried at 105 °C until constant weight, then, bonded on the sample holders with conducting glue carbon. The morphologies of the products are observed at microscopic level.

3. Results and Discussion:

3. 1. Electrical conductivity:

The measurement of electrical conductivity is accurate and reproducible method, can give an important information about the physico-chemical changes taking place during hydration especially at early age period [18]. Electrical conductivity of GBFS-SF pastes containing different contents of SF namely, 2, 4, and 8 mass% SF was given in Fig. 8.

Fig. 8 showed that the electrical conductivity time curve from 20 min up to 28 days. Electrical conductivity of alkaline activated GBFS-SF pastes show a higher maxima at early ages (0 time). The electrical conductivity maxima at initial time increases, this is due to free OH^- and Na^+ ions were released from the pores of the fresh paste. These ions act as charge carriers, leading to rapid increase in the conductivity maximum. Once the concentration of these ions in the solution become very high, ionic association starts taking place, then concentration of ions starts to decrease as shown after 20-30 min. This occurs during the induction period and the conductivity decreases. During this period, some of these ions adsorbed and precipitated with the formation of C-S-H, C-A-H and C-A-S-H hydrates [19], forming electrical double layer or protective film leading to the decrease in the mobility of ions. Increase the contents of SF the electrical conductivity maxima decreases, due to the high surface area and high pozzolanity of SF. Presence of 2 mass% SF shows a slight shift in the electrical conductivity peaks to longer hydration time, this is due to the fact that SF forms assort of coating around GBFS particles during the early stages of the hydration process. GBFS-SF mixes suffer from a sharp decrease in electrical conductivity maxima during hydration periods, with the increase of SF contents up to 8 mass%.

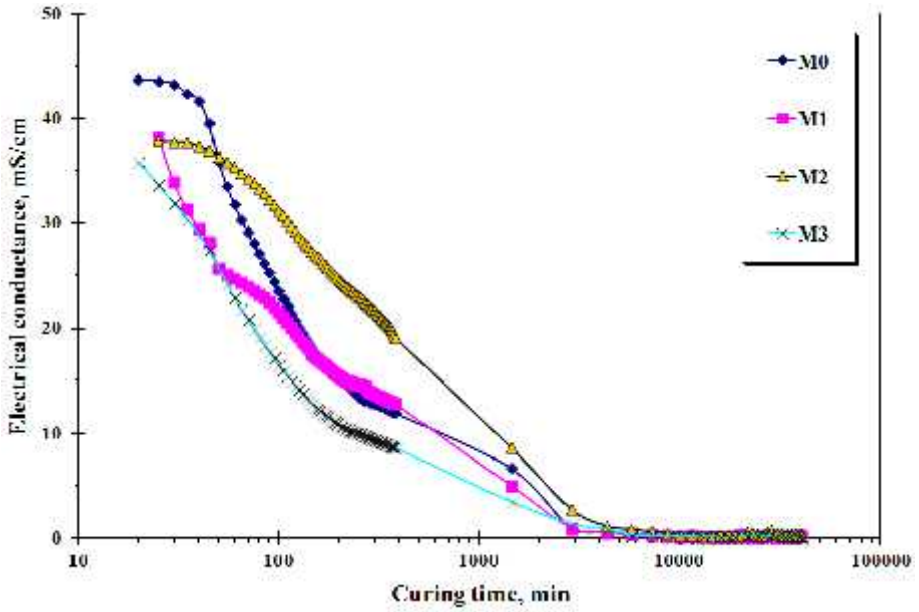

Fig 8: Electrical conductivity of alkali activated GBFS-SF as a function of curing time.

3.2. Chemically combined water contents:

The chemically combined water contents of alkali activated GBFS-SF pastes cured up to 90 days in tap water are graphically plotted as a function of curing time in Fig. 9. The chemically combined water content increases gradually with curing time for all hydrated alkaline activated GBFS-SF pastes, this is due to the progress of the hydration process and the amount of hydration products increase. The chemically combined water contents of mix M2 gives the higher values at all curing ages. The decrease of combined water of mix M3 is mainly due to the formation of more C-S-H with lower water content than that formed from the activation of GBFS. The activation of GBFS pastes give calcium silicate hydrate in addition to calcium aluminate hydrate and gehlenite-like hydrate. The chemically combined water contents increases up to 4 mass% of SF, then decreases with the increase of the contents of SF up to 8 mass%. The decrease in chemically combined water contents is due to the SF may form a coated film on GBFS grains. The increase of chemically combined water contents in the presence of 4 mass% of SF may be due to the higher pozzolanicity of SF, which reacts to form hydrated products such as C-S-H, C-A-H and C-A-S-H. On the other hand, increase of the addition of SF (>4 mass, %) decreases the combined water content [20].

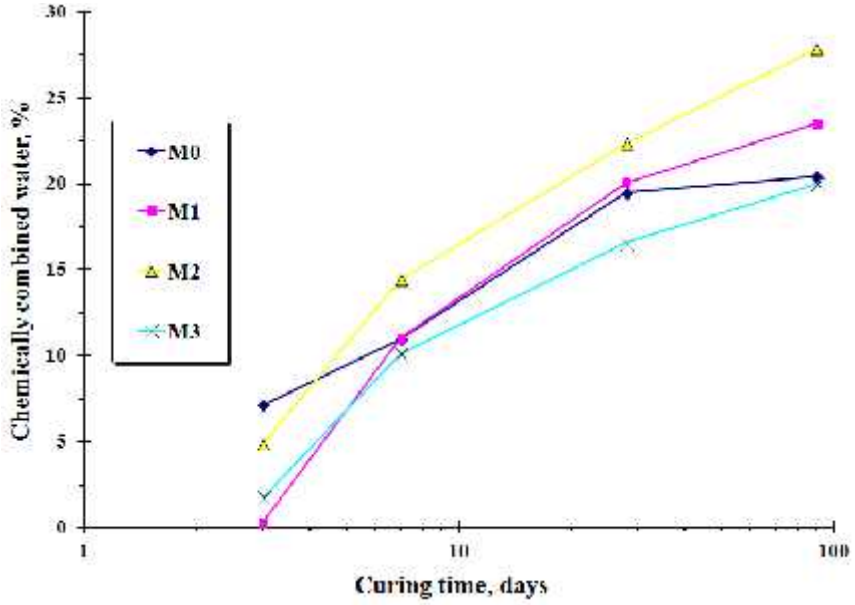

Fig 9: Chemically combined water contents of alkali activated GBFS-SF up to 90 days.

3.3. Combined slag contents:

The results of combined slag contents of alkali activated GBFS-SF pastes are graphically plotted as a function of curing time up to 90 days in Fig. 10. It is clear that the combined slag contents for all mixes increase with curing time. The combined slag content increases with curing ages up to 90 days. Combined slag content increases with SF contents up to 4 mass%. SF reacts with OH^- giving C-S-H as well as Na-silicate hydrate (N,C)-A-S-H gel. Therefore, as the amount of SF increases can be react with activator, to decrease the combined slag content. Increase of SF content up to 8 mass% the combined slag content decreases.

3.4. Compressive strength:

Compressive strength values of hardened alkali activated GBFS-SF mixes containing different contents of SF up to 8 mass% as a partial replacement of GBFS cured for 3, 7, 14, 28 and 90 days are graphically represented as a function of curing time in Fig. 11. The results show that the compressive strength increases with curing time for all hardened activated GBFS-SF pastes. This is due to the progressive of hydration products, forming C-S-H, C-A-H, C-A-S-H and (N,C)-A-S-H gel leading to form close compact and homogeneous structure. The results also indicated that the increase in compressive strength with the increase in SF contents up to 4 mass%. With the increase in SF content up to 8 mass% compressive strength shows a lower values. But, at later age up to 28-90 days, the compressive strength increases. The compressive strength increases with SF content up to 4 % is due to highly effective pozzolanic activity of SF or acts as nucleating agents or as a seeding for formation of C-S-H gel.

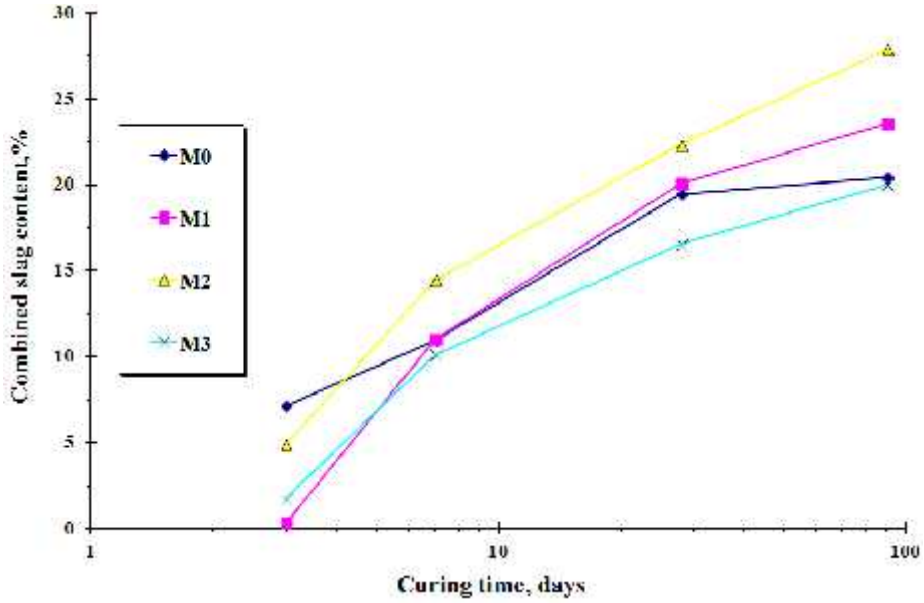

Fig10: Combined slag contents of alkali activated GBFS-SF mixes up to 90 days.

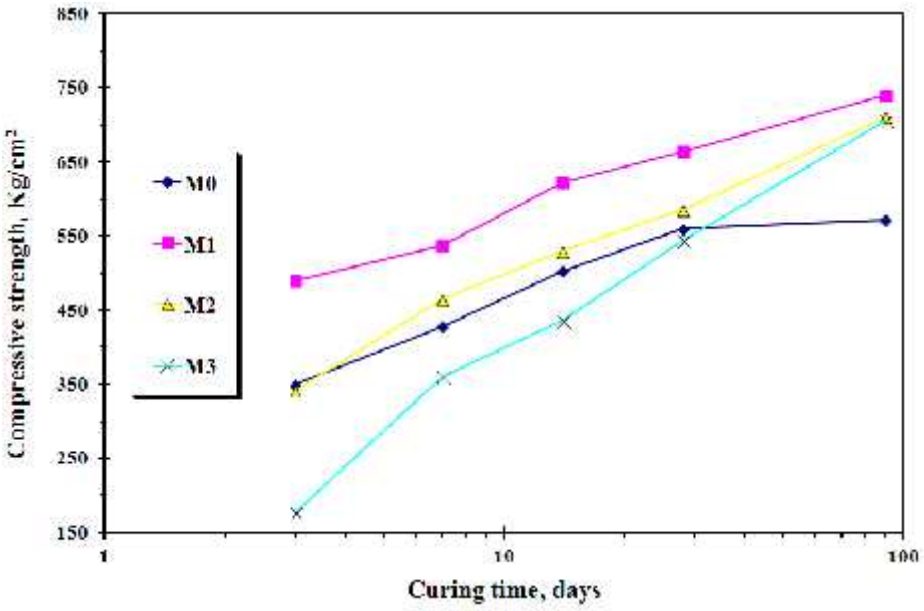

Fig 11: Compressive strength of alkaline activated GBFS-SF as a function of curing time up to 90 days.

3.5. Bulk density:

The bulk density of alkali activated GBFS-SF mixes containing different contents of SF up to 8 wt % cured for 3, 7, 14, 28 and 90 days are graphically plotted as a function of curing time in Fig. 12. It is clear that the bulk density for all hardened alkali activated GBFS-SF pastes increased with curing time. This is due to the continuous hydration and precipitation as well as accumulation of the hydrated products filling up the available pore as a result the bulk density values increase. The bulk density of mix M0 is the lowest values while the values of mix M1 are the highest values at all curing times, this is due to the presence of SF, which modifying the hydration products as well as increases the amount of calcium silicate hydrate. Alkaline activator accelerates the dissolution of Si and Al ions by breaking the Si-O and Al-O bonds in slag glass structure which is followed by precipitation of low-solubility calcium silicate, calcium aluminate and magnesium aluminate hydrates [21]. SF modifies the hydration products as well as increases the amount of calcium silicate hydrate.

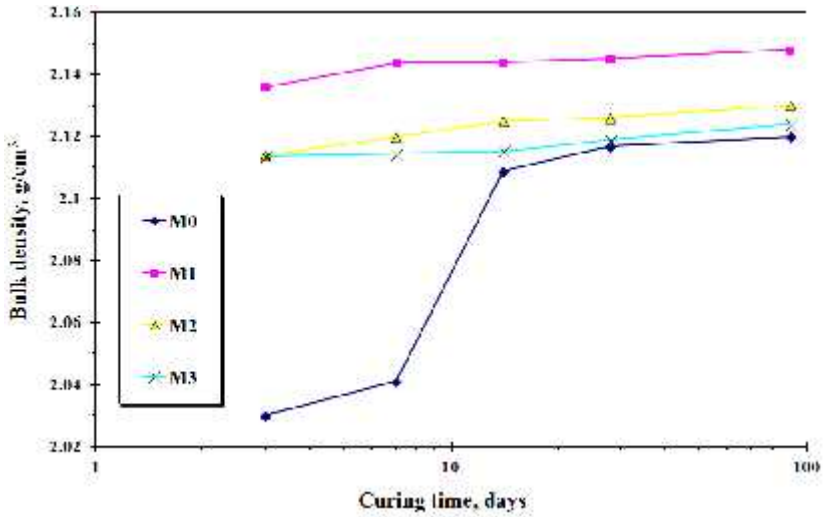

Fig 12: Bulk density of alkali activated GBFS-SF mixes as a function of curing time up to 90 days.

3.6. Total porosity:

The total porosity values of alkali activated GBFS-SF pastes containing different dosages of SF cured for 3, 7, 28, and 90 days are graphically plotted as a function of curing time in Fig. 13. It is clear that the total porosity decreases till the minimum value for all mixes at 90 days. Mix M0 has the higher values of total porosity while mix M1 has the lowest values. These results indicate that the hydration reactions precipitated and accumulated gradually to filling up the available pore volume till reach the minimum values at 90 days. The presence of SF in the mixes causes considerable reduction in the volume of large pores at all ages. SF acts as filler due to its fineness higher surface area, which it fits into spaces between grains in the same way that sand fills the spaces between particles of coarse aggregates and fill the spaces between fine grains [22].

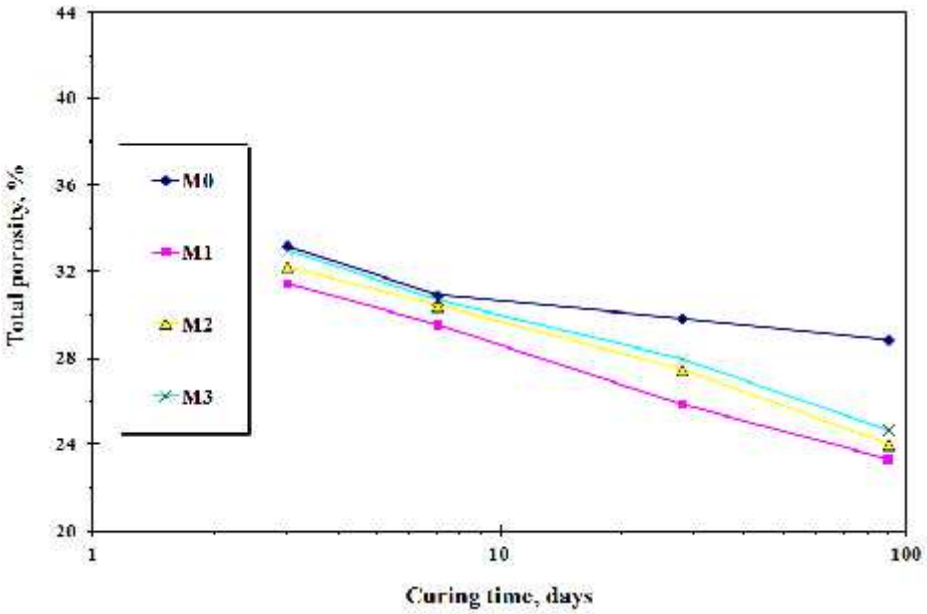

Fig13: Total porosity of alkali activated GBFS-SF mixes as a function of curing time up to 90 days.

3.7. Thermo-gravimetric analysis:

Fig. 14 presents thermograms of mix M2 alkali activated with (0.75:0.50;Na_2O:SiO_2 mol/kg of GBFS-SF), which cured for 3, 28 and 90 days. The weight loss at 1000 ^oC was found to be 4.398%, 8.861 and 11.950% for 3, 28 and 90 days,

respectively. The increase in weight loss is related to the progress of geopolymerization process. The dissolution process in alkaline medium implies that Si–O–Si, Al–O–Al and Si–O–Al bonds are broken, yielding Al–OH and Si–OH groups. In the geopolymerization process, part of these new groups are arranged (condensation reaction) to form new Si–O–Al bonds. However, some of the Si–OH and Al–OH groups remain unreacted. The weight loss observed in TGA for geopolymerized paste is attributed to the decomposition (water loss) of these Si–OH groups and Al–OH groups. The endothermic peak located at 60-90 °C is due to the dehydration of free and interlayer water of C-S-H. The weight loss due to the dehydration of interlayer water of C–S–H was 2.20%, 4.735% and 7.97% for the pastes cured after 3, 28 and 90 days, respectively. The endothermic peaks located below 200 ^{o}C is related to C–A–H and C–A–S–H. A general increase in weight loss with curing time is observed, which may be associated with a greater degree of alkaline activation [23]. The weight loss generally increases with Na^{+} concentration, can be related to a higher degree of chemically bounded water and OH^{-} groups, provided alkaline activation, in the binding phase. The exothermic peak located at 850-870^{o}C is attributed to the crystallization of the pseudo-wollastonite phase (monocalcium silicate, CS). Exothermic peak is characteristic for the decomposition of C–S–H [24].

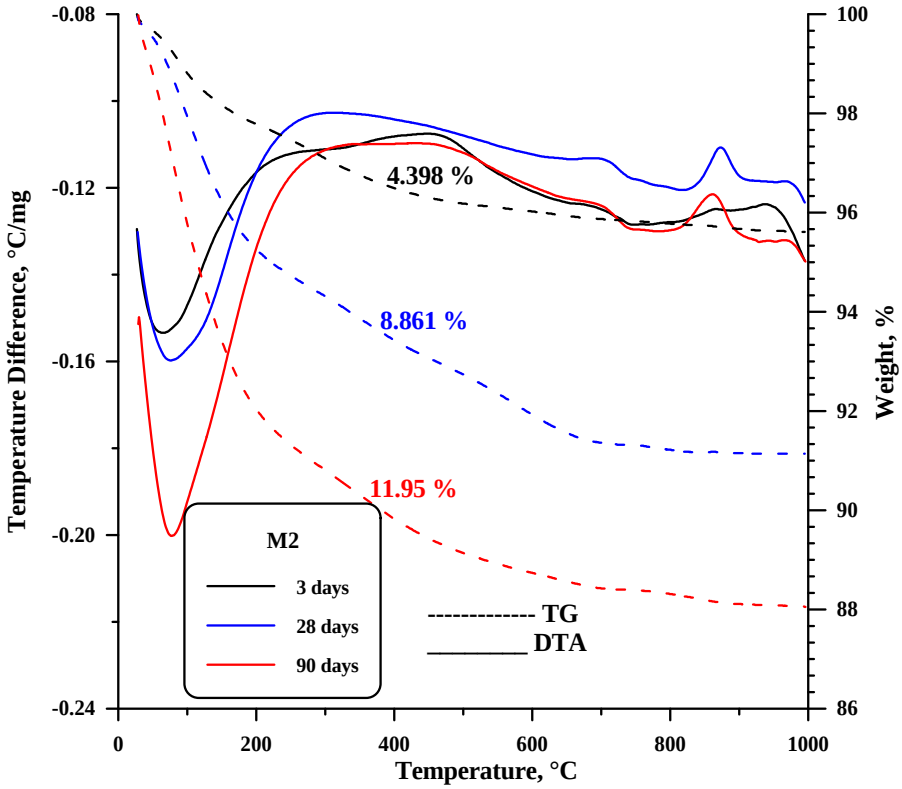

Fig14: DTA/TG thermograms of mix M2 activated cured up to 90 days.

3.8. X-ray diffraction:

Fig. 15 presented the XRD patterns of alkali activated M2 mix containing 4 mass% of SF as the partial replacement of GBFS cured up to 90 days. It can be observed that the hump peak in the range of 20–38^{o} 2θ changes with curing time from 1 day up to 90 days. XRD patterns illustrate the increase in calcite content. SF has higher specific surface area in interacting with dissolved calcium from GBFS forming C-S-H. The peak of X ray diffraction pattern corresponding to C-S-H overlap with that of calcite. SF has a positively affect on the geopolymerization process by acting as a nucleation centers for the formation and accumulation of the geopolymer [25].

3.9. Fourier transformation infrared spectroscopy:

FT-IR spectra of alkaline activated M2 mix are shown in Fig. 16. The broad band located at 3448 and 3449cm^{-1} are assigned to stretching vibration of O-H. The bonding vibration frequency of H-O-H lattice in C-A-H and C-A-S-H hydrated are located at 1507, 1637, and 1638cm^{-1}. The observed band at 1458, 1466, and 1489 cm^{-1} are due to the stretching vibration

of C-O bond in CO_3, which results from the carbonation of hydrated products. Its intensity decreases with curing time, due to the increase of bulk density and hindrance of carbonation of the hydrated samples [26].

The band at around 1116, 1019 and 1010cm^{-1} are due to T-O-Si (T: Si or Al) asymmetric stretching vibration as a result of TO_4 reorganization that takes place during synthesis [27]. The stretching in the region of 875 cm^{-1} is due to Si-O stretching. The band at 477, 461 and 457 cm^{-1} is due to binding vibration of Si-O-Si and O-Si-O [25].

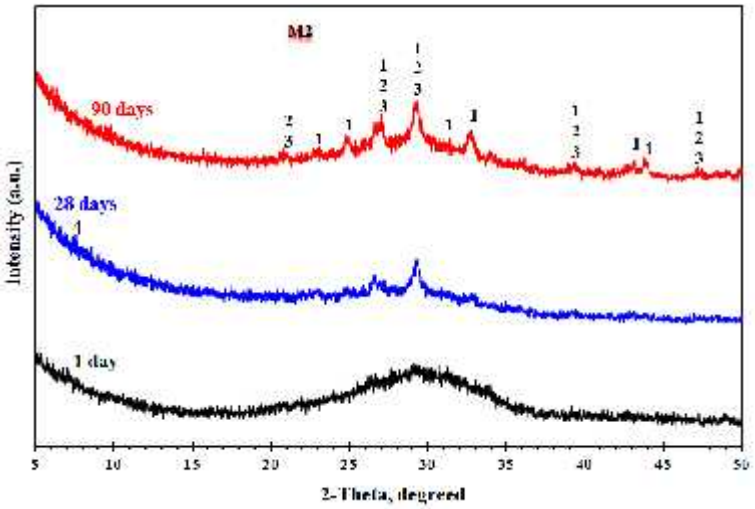

Fig15: XRD pattrens of mix M2 activated with (0.75:0.50; Na_2O:SiO_2mol/kg) cured up to 90 days, (1. Calcite; 2.Wollastonite; 3. Calcium silicate hydrate; 4. Tobermorite).

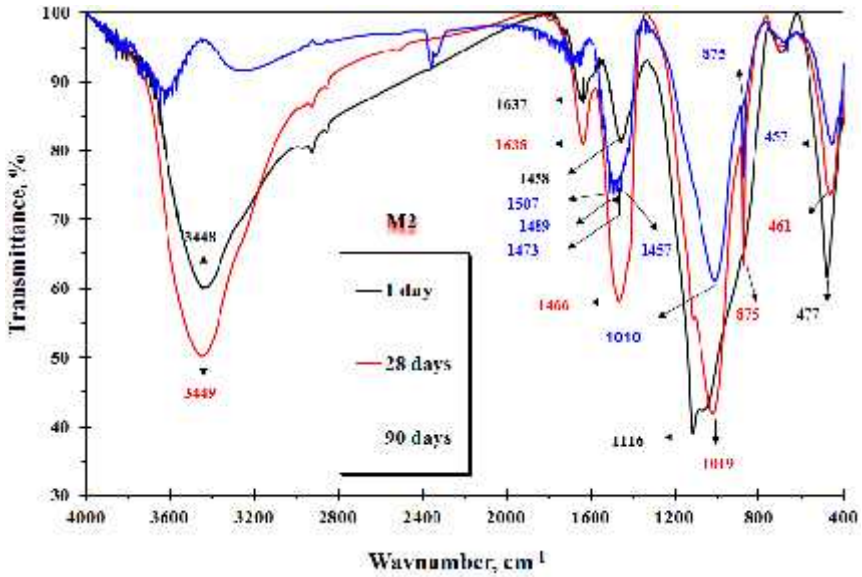

Fig16: FTIR of mix M2 cured up to 90 days.

3.10. Scanning electron microscopy:

The microstructure development of alkali activated GBFS-SF mix M2 was analyzed by using SEM images at 3 and 90 days. Fig. 17 shows SEM micrograph of M2 sample hydration at 3 and 90 days. The micrograph of mix M2 hydrated at 3 days shows the presence of amorphous film of C-S-H (III) covered the surface of specimens. At 90 days, the micrograph showed the presence of C-S-H with different morphologies, and a new feature as C-S-H type I, with fibrous acicular morphology [28]. SF enhances the formation of fibrous structure of C-S-H with denser spheres [28-31] as represented in Fig.

17, these compact structure of C-S-H leads to enhancement the microstructure performance providing an additional increase in strength of the sample containing SF. SF forms additional nucleation or polymerization-condensation centers for the precipitation of geopolymer as indicated from the morphology, where a massive platy geopolymer layer fill mostly the matrix composition.

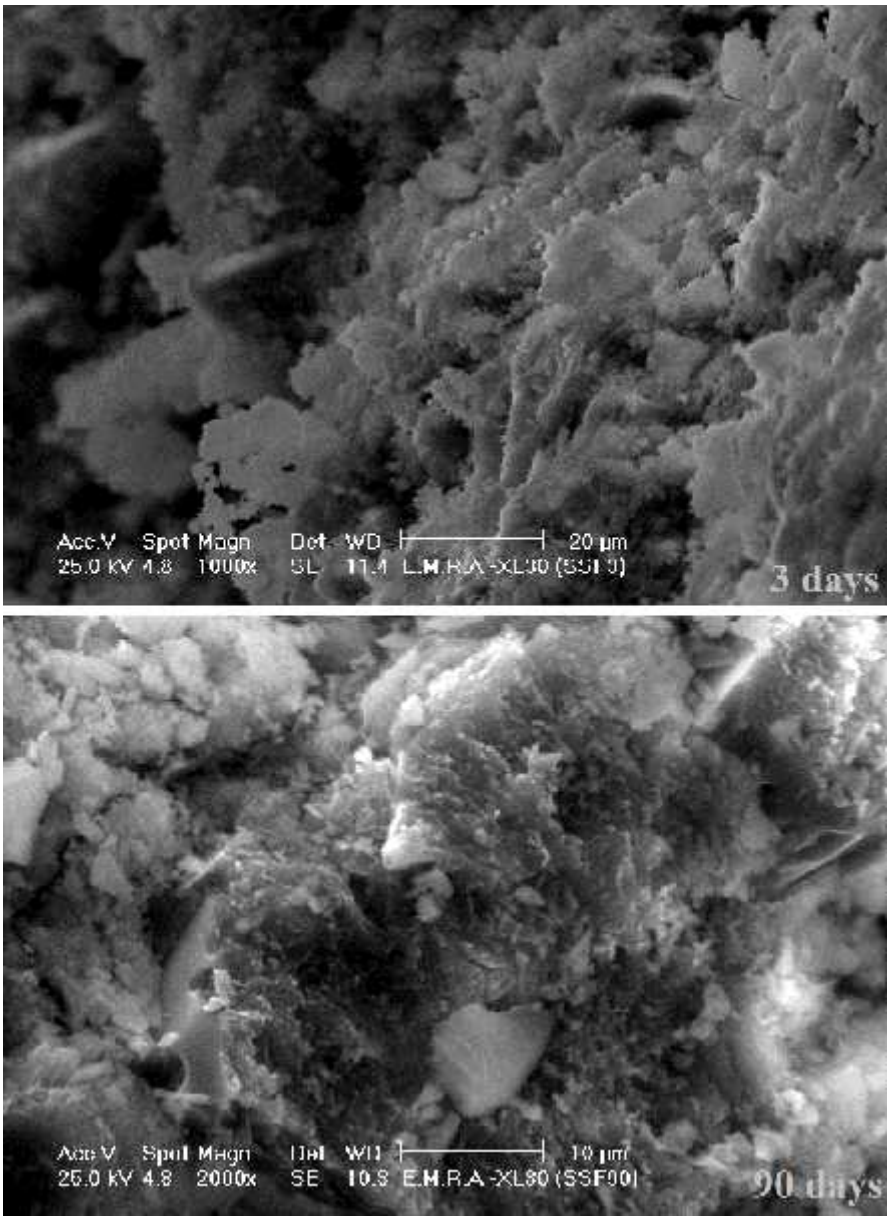

Fig 17: SEM micrograph of mix M2 cured up to 3 and 90 days.

3.10. Resistance to aggressive attack:

3.10. 1. Magnesium sulphate solution:

Magnesium sulphate has a more aggressive attack than sodium sulphate because $MgSO_4$ decomposes the calcium silicate hydrates during long-term exposure to produce magnesium silicate hydrates and CH. Hydrated magnesium silicate has no binding properties [15]. Chemical attack by aggressive magnesium sulphate is one of the factors responsible for damaging cement matrix. This aggressive behavior increases with increasing sulphate ions in the cement paste can enter into deleterious chemical reactions [32,33].

3.10.1.1. Compressive strength:

The compressive strength of alkali activated M0, M2 as well as OPC cement pastes immersed in 5% $MgSO_4$ solution up to 180 days are graphically plotted in Fig. 18. The compressive strength of alkaline activated GBFS increases with curing time as the hydration progresses up to 180 days. The compressive strength of mix M2 shows the higher values, due to a good pozzolanic activity in alkaline activation that exhibits higher resistance to sulphate medium up to 180 days. The compressive strength of alkaline activated GBFS paste increases in the presence of 4 mass% SF due to the formation of additional C-S-H hydrates which deposited in the available pores and hence decreases the porosity. SF showed a good pozzolanic activity in alkaline activation to form $n_1CaO.SiO_2.n_2H_2O$ (C-S-H) which responsible for the strength and lowering the pore volume [34]. The compressive strength of OPC pastes immersed in 5% $MgSO_4$ increases up to 90 days then decreases [15,35,36]. The decrease of compressive strength of OPC pastes after 180 days is mainly due to the presence of high values of alite and belite, which liberate $Ca(OH)_2$ that forms ettringite [15,35,36]. The liberated CH available in the hydrated OPC cement pastes matrix get reacted with 5% $MgSO_4$ resulting the formation of gypsum as well as the calcium aluminate phases of both hydrated and the unhydrated portions of cement in the matrix, leading to formation of ettringite which is an expansion creating compound, these phases expand the cement pastes [37-39]. By comparing the alkali activated GBFS with OPC cement pastes, it is found that the strength of alkali activated slag increases up to 180 days, due to the formation of C-S-H and geopolymer [40].

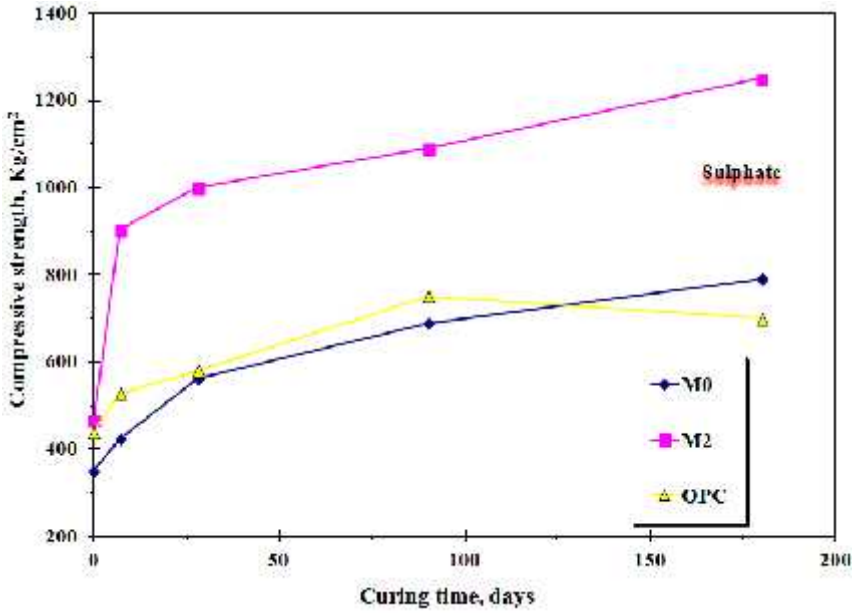

Fig18: Compressive strength of activated GBFS-SF and OPC pastes subjected to 5% $MgSO_4$ solution up to 180 days.

3.10.1.2. Total sulphate content:

The total sulphate content of alkali activated mixes (M0, M2) as well as OPC cement pastes immersed in 5% $MgSO_4$ solution up to 180 days are graphically represented in Fig. 19. The values of total sulphate contents increase with the immersing time due to immersion of pastes in aggressive medium containing sulphate ions (5% $MgSO_4$). The resistivity towards sulphate solution increases with SF content.This is mainly due to the decrease in the total porosity hinders the penetration of sulphate ions in the binder matrix. OPC pastes give higher values of total sulphate content than those of alkali activated binder.

3.10. 2. Magnesium chloride solution:

The corrosive action of chlorides is due to the formation of chloroaluminate hydrates, which causes softening of concrete. The chlorides attack proceeds by ionic penetration of Cl^- into concrete. This penetration is independent of the chloride concentration and concrete penetrability. Diffusion seems to be dependent not only on the porosity of the matrix but also on the nature of the paste. Moreover, Cl^- ionic diffusion depends not only on the permeability and binding capacity of Cl^- ions, but also on the ion-exchange capacity of the system.

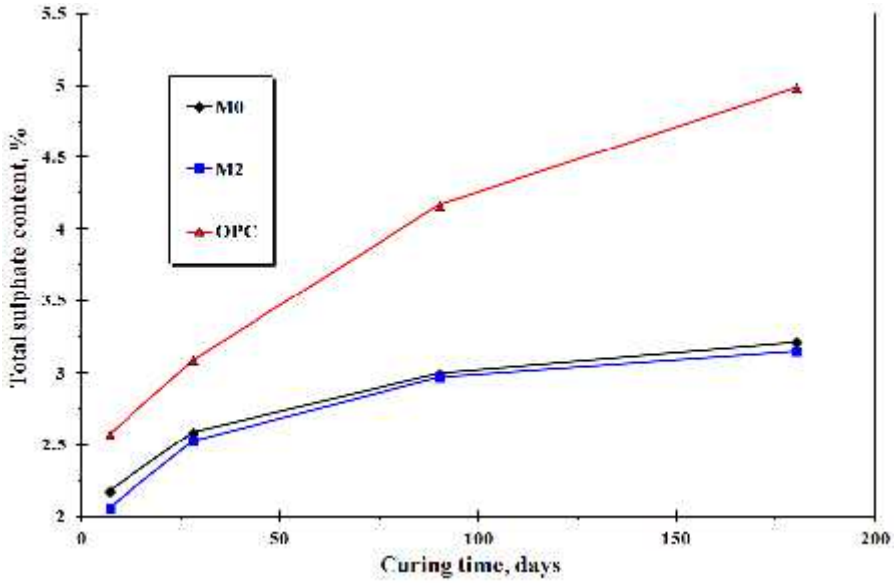

Fig19: Total sulphate of activated GBFS-SF and OPC pastes subjected to 5% $MgSO_4$ solution up to 180 days.

3.10. 2.1. Compressive strength:

The compressive strength values of alkaline activated M0, M2 as well as OPC cement pastes immersed in 5% $MgCl_2$ solution up to 180 days are graphically represented in Fig. 20. The compressive strength increases with curing time; this is due to the continuous hydration. This increase in compressive strength values,this is due to the promotion of hydration products with curing time due to the adsorption and incorruption of a part of Mg^{2+} ions onto the C-S-H particles which enhance the crystallization of C-S-H [41]. OPC contains free CH content in its matrix due to its hydration reactions, this free lime and the hydrated OPC matrix (C-S-H gel) are easily attacked by acids in general [35,37,42]. The compressive strength of mix M0 increases gradually up to 180 days due to good resistance to chloride medium, whereas, the values of compressive strength of OPC shows a lower values from 28 days up to 180 days. Replacement 4 mass % of GBFS with SF (mix M2) increases the values of compressive strength than neat GBFS. SF has higher surface area and high pozzolanic activity values, which enhanced with the action of alkaline activator. SF decreases the total porosity, hence increases the durability of GBFS-SF binder. M2 gives the higher values of compressive strength than all investigated binders, due to the formation of a denser structure enhances the durability to chloride medium up to 180 days.

3.10. 2.2. Total chloride content:

The total chloride contents of alkali activated M0, M2 as well as OPC cement pastes immersed in 5% $MgCl_2$ solution up to 180 days are graphically plotted in Fig. 21. The total chloride content increases with curing time for all mixes up to 180 days. The total chloride sharply increases after first week up to 28 days, then it slowly increases up to 180 days for all pastes. The increase in total chloride contents of OPC up to 180 days is mainly is due to the reaction of $MgCl_2$ with CH forming $CaCl_2$ and $Mg(OH)_2$. $CaCl_2$ reacts with C_3A and/or C_4AF to form chloroaluminate hydrate ($C_3A.CaCl_2.10H_2O$). Also, $MgCl_2$ reacts also with C-S-H hydrates to form calcium chloride, magnesium hydroxide and silica gel. The alkali activated GBFS do not have free lime content in its matrix and geopolymers themselves are not easily attacked by aggressive medium containing [43]. This is mainly due to the accumulation of excessive amounts of hydrates within the pore systems at larger hydration times. The total chloride content decreases due to the formation of additional hydrated calcium silicates that fill some available open pores which in turn improves the microstructure of the system thereby inhibits the chloride ions penetration. This effect leads to a decreased accessibility of chloride ions towards the more dense with low capillary pore structure of the hardened pastes on the prolonged hydration. While M2 have the lower chloride contents up to 180 days immersion in $MgCl_2$ solution due to lower diffusion of chloride through the pastes with SF content. The decrease of the diffusion of chloride ions are attributed to the decrease of the total porosity as a result of the precipitation of more hydration products formed from the pozzolanic activity of SF to form additional C-S-H.

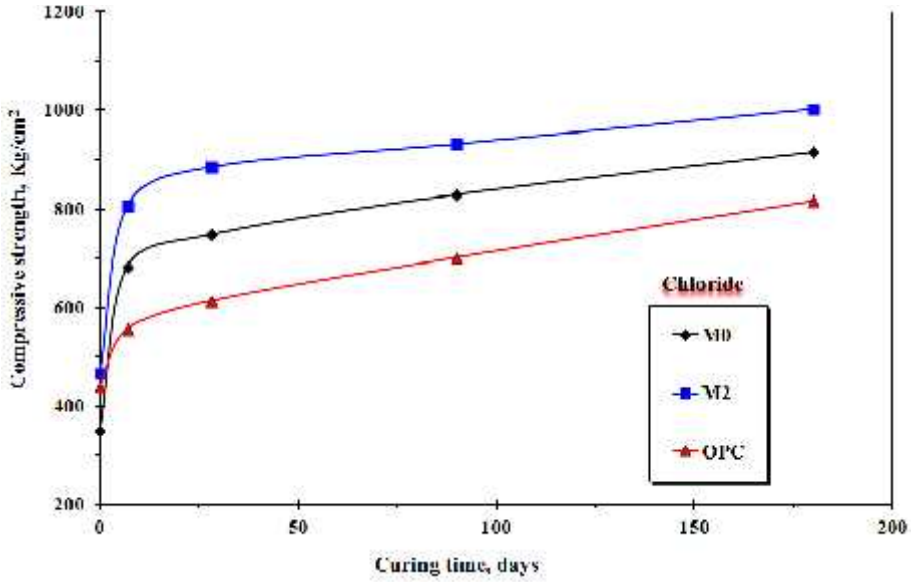

Fig. 20: Compressive strength of activated GBFS-SF and OPC pastes immersed in 5% $MgCl_2$ solution.

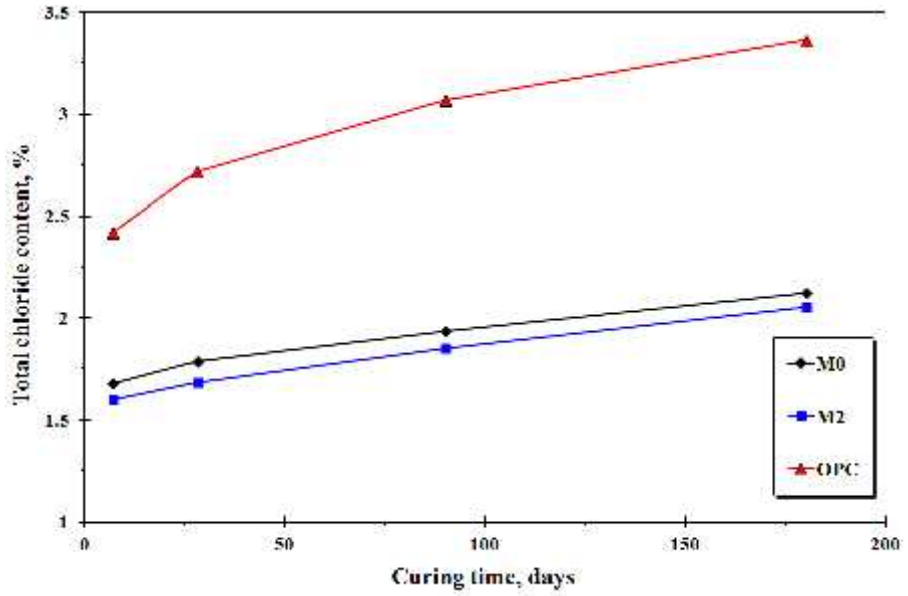

Fig 21: Total chloride of activated GBFS-SF pastes as well as OPC immersed in 5% $MgCl_2$ solution.

4. Conclusions:

The main conclusions could be derived from this investigation are summarized as follows:

1. GBFS-SF mixes suffer a sharp decrease in electrical conductivity maxima during hydration periods.The presence of 2 mass% of SF shows a slight shift in the electrical conductivity peaks to longer hydration time.
2. The chemically combined water contents of mix M2 gives the higher values at all curing ages.
3. The combined slag content increases with SF contents up to 4 mass%.
4. Mix M1 shows the higher values of compressive strength at all curing ages of hydration. The increase in compressive strength is due to higher surface area and effective pozzolanic activity of SF, it acts as nucleating agents or as a seeding for formation of C-S-H gel.
5. The compressive strength of mix M2 shows a higher value, this is due to a good pozzolanic activity in alkaline activation, which exhibits higher resistance to sulphate and chloride aggressive solutions up to 180 days.

6. The total sulphate and chloride contents of alkali activated mix M2 shows a lower values of sulphate or chloride contents when immersion in 5% $MgSO_4$or 5% $MgCl_2$solutions.
7. It can be concluded that alkali activated GBFS-SF are more durable in 5% $MgSO_4$ or 5% $MgCl_2$than OPC pastes.

References

1. M. Sayed, S.R. Zeedan, Housing and Building National Research Center, 8 (2012) 177–184.
2. R.Siddique, 2008, Springer-Verlag Berlin Heidelberg, (2008)1-40.
3. H.Uchikawa, Principal Report (Brazil), 1 (1986) 249–280.
4. V.M. Malhotra, V.S. Ramachandran, R.F.Feldman, P.C.Aitcin, Boca Raton, Florida: CRC Press, Inc 1987.
5. S.D.Wang, K.L. Scrivener, Concrete Research, 33 (2003) 769-774.
6. V. Glukhovsky, Kiev. Ukraine, 1 (1994) 1-8.
7. P.D.Krivenko, Kiev, Ukarine1994.
8. A. Fernandez-Jimenez, F. Puertas, I. Sorbrados, J. Sanz, Journal of American Ceramic Society, 86 (2003) 1389–1394.
9. A. Fernandez-Jimenez, F. Puertas, Advanced Cement Research, 13 (2001) 115-121.
10. N.Y. Mostafa, S.A.S. El-Hemaly , S.A. El-Wakeel, S.A. El-Korashy, P.W. Brown, Cement and Concrete Research, 31 (2001) 899-904.
11. M.C.G. Juenger, C.P. Ostertag, Effect Concrete Science and Engineering, 4 (2002) 91–97.
12. American Society for Testing and Materials American Society for Testing and Materials, ASTM Standards, Standard Test Method for Normal consistency of Hydraulic cement, American Society for Testing and Materials, C 187-83, 2008;195.
13. M. Heikal, I. Aiad, I.M. Helmy, Portland cement clinker, granulated slag and by-pass cement dust composites, Cement and Concrete Research, 32 (2002) 1805-1812.
14. M. Heikal, M.S. Morsy, M.M. Radwan, Cement and Concrete Research, 35 (2005) 1438-1446.
15. M. A. Abd- El Aziz, M. Heikal, Advances in Cement Research, 21 (2009) 91-99.
16. M. Heikal, M.S. Morsy, E. El-Shimy, S.A. Abo-El-Enein, l'industriaitaliana del Cemento (iiC) (7-8) (2004) 614-625.
17. J. Stark, H.M. Ludwing, A. Müller, ZementKalkGips, 90 (1991) 557-560.
18. F. D. Tamás, cement and Concrete Research, 12 (1982) 115-120.
19. M.M. Tashima, L. Soriano, M.V. Borrachero, J. Monzó, J. Payá, Bulletin of Material Science, 36 (2013) 245–249.
20. A. Kar , I. Ray , A. Unikrishnan , F. Davalos , Cement and Concrete Composites, 34 (2012) 419–429.
21. X. Wu, W. Jiang, D.M. Roy, Cement and Concrete Research, 20 (1990) 961-974.
22. R. Siddique, M.I. Khan, Engineering Materials, Ch:2, Springer-Verlag Berlin Heidelberg, (2011) 67-119.
23. M.M. Tashima, J.L. Akasaki, V.N. Castaldelli, L. Soriano, J. Monzó, J. Payá, Materials Letters, 80 (2012) 50–52.
24. V.S. Ramachandran, R.M. Paroli, J.J. Beaudoin, A.H. Delgado, William Andrew Publishing Norwich, New York, U.S.A., (2002) p.692.
25. H.M. Khater, International Journal of Advanced Structural Engineering, (2013) 5-12.
26. M. Heikal, S. Abd El Aleem, W.M Morsi, 9 (2013) 243-255.
27. J.A. Gadsden, Butterworths, London 1975.
28. S. Diamond, Rio de Janeiro, Brazil, (1986) 122–147.
29. H.F.W. Taylor, *Cement chemistry*. 2nd edition. London: Academic Press; 1992.

30. V.M. Malhotra, P.K. Mehta, Pozzolanic and cementitious materials, vol*1*. Ottawa: Overseas Publishers Association; 1996.

31. P.J.P. Gleize, A. Müller, H.R. Roman, Cement and Concrete Composites, 25 (2003) 171-175.

32. M. Sahmaran, O. Kasap, K. Duru, I.O. Yaman, Cement and Concrete Composites, 29 (2007) 159-167.
33. S.U.Al- Dulaijan, Building Materials, 21 (2007) 1792-1802.

34. K.S. Wang, K.L. Lin, Z.q. Huang, Cement and Concrete Research, 31(2001) 97-103.

35. H. El-Didamony, A.A. Amer, H. Abd El-Aziz, Ceramics International, 38 (2012) 3773–3780.

36. M. Abd El-Aziz, S. Abd El-Aleem, M. Heikal, H. El-Didamony**,** Cement and Concrete Research, 35 (2005) 1592-1600.

37. W.G. Hime, B. Mather, Cement and Concrete Research, 29 (1999) 789-791.

38. P.C. Hewlett Technology & Engineering), (2003)p.1092.

39. P. Dinakar, K.G. Babu, M. Santhanam, Cement and Concrete Composites, 30 (2008) 880-886.

40. C. K. Yip, G. C. Lukey, J. L. Provis, J.S.J. Van Deventer, Cement and Concrete Research, 38 (2008) 554–564.

41. M. Heikal, M.A. Abd El-Aziz, Advances in Cement Research, 21 (2009) 91-99.

42. A. Hajimohammadi, J.L. Provis, J.S.J. van Deventer, Journal of Colloid and Interface Science, 357 (2011) 384–392.

43. T. Bakharev, J.G. Sanjayan, Y.B. Cheng, Cement and Concrete Research, 33 (2003)1607–1611.